CHEMISTRY
A EUROPEAN JOURNAL

ChemPubSoc
Europe

DOI: 10.1002/chem.201204298

Pyrrolic Tripodal Receptors for the Molecular Recognition of Carbohydrates: Ditopic Receptors for Dimannosides

Oscar Francesconi,[b] Cristina Nativi,[b] Gabriele Gabrielli,[b] Matteo Gentili,[b] Marco Palchetti,[b] Beatrice Bonora,[b] and Stefano Roelens*[a]

Abstract: Synthetic ditopic receptors, designed for the molecular recognition of dimannosides, have been prepared by bridging two monotopic units effectively recognizing mannosides with linkers of the appropriate size and flexibility, endowed with hydrogen-bonding groups. Affinities toward the α and β glycosides of the biologically relevant Manα(1–2)Man disaccharide were measured by NMR spectroscopy and isothermal titration calorimetry (ITC) in polar organic media (30–40% DMF in chloroform). Significant selectivities and affinities in the micromolar range were observed in most cases, with two newly designed receptors being the most effective receptors of the set, together with a distinct preference of the dimannosides for the (*S*) enantiomer of the receptor in all cases. A 3D view of the recognition mode was elucidated by a combined NMR spectroscopic/molecular modeling approach, showing the dimannoside included in the cleft of the receptor. Compared to the monotopic precursors, the ditopic receptors showed markedly improved recognition properties, proving the efficacy of the modular receptor design for the recognition of disaccharides.

Keywords: binding · carbohydrates · mannosides · molecular recognition · synthetic receptors

Introduction

Molecular recognition of carbohydrates has become a topic of high interest in the past decade. The impetus for research in this field is largely provided by the prominence of carbohydrate recognition events in biological processes,[1] which stimulated the development of artificial biomimetic receptors,[2] not only to mimic the natural receptors and to understand recognition mechanisms in biological systems, but also to develop new therapeutic and diagnostic tools for medicine and technology.

In biological systems, carbohydrate recognition is exerted by dedicated classes of biomolecules, such as lectins and antibodies, which govern the interaction between living cells and other cells or pathogens through the specific recognition of the saccharidic chains of glycoconjugates exposed on cell or pathogen surfaces.[1c] The epitopes involved in the recognition processes are usually the terminal mono- or oligosaccharides, among which mannosides are frequent and play a central role in both pathological and therapeutic processes. Indeed, mannosides are recognized by a variety of lectins[3] and are involved in infections caused by several high-risk pathogens, like pathogenic yeasts (Candida),[4] bacteria (micobacterium tubercolosis),[5] and viruses (HIV and Hepatitis HCV).[6] On the other hand, antibodies, such as 2G12[7] or PGT128,[8] lectins, such as cyanovirin-N,[9] microvirin,[10] or actinohivin,[11] and other natural non-peptidic molecules, such as benanomicin A and pradimicin A,[12] which show potent antiviral activity, owe their antiviral properties to the specific recognition of terminal oligomannosides on the pathogen surface.

A particularly relevant example of pathological consequences of mannose recognition is the binding of the DC-SIGN lectin of the immune system dendritic cells to the viral glycoprotein gp120 on the HIV envelope, which triggers the infection of human cells by HIV.[13] In this binding event, the Manα(1–2)Man dimannoside motif is the smallest fragment of the Man9 epitope of the gp120 glycans required for recognition by the DC-SIGN lectin.[14]

It thus appears that oligomannosides are targets of high interest in the design of artificial receptors, especially in the search for effective carbohydrate binding agents (CBAs) for therapeutic purposes.[13] However, the endeavor dedicated to the design of structures for the recognition of carbohydrates has been so far focused mainly on monosaccharidic targets, to an extent that examples of biomimetic receptors selectively recognizing oligosaccharides through noncovalent interactions are still rare.[15] Most remarkably, although receptors showing preference for the most commonly availa-

[a] Dr. S. Roelens
Istituto di Metodologie Chimiche (IMC)
Consiglio Nazionale delle Ricerche (CNR)
Dipartimento di Chimica, Università di Firenze
Polo Scientifico e Tecnologico, Via della Lastruccia, 13
50019 Sesto Fiorentino, Firenze (Italy)
Fax: (+39) 055-457-3570
E-mail: stefano.roelens@unifi.it

[b] Dr. O. Francesconi, Prof. C. Nativi, Dr. G. Gabrielli, M. Gentili, M. Palchetti, B. Bonora
Dipartimento di Chimica, Università di Firenze
Polo Scientifico e Tecnologico
50019 Sesto Fiorentino, Firenze (Italy)

Supporting information for this article is available on the WWW under http://dx.doi.org/10.1002/chem.201204298.

ble cellobiose, maltose, lactose, and sucrose saccharides have been reported, displaying excellent recognition properties in some cases,[15a] to the best of our knowledge, we are not aware of any report on the recognition of dimannosides or oligomannosides through synthetic receptors.

In the course of our studies on the design of biomimetic receptors for carbohydrates, we have described a family of aminopyrrolic tripodal structures showing the highest affinities and selectivities for α- and β-mannosides reported to date.[16] Due to the biological significance of oligomannosides, the results obtained encouraged us to further explore the recognition of dimannosidic targets by adjusting the architecture of our mannose-selective receptors.

We would like to describe here the successful design of a new generation of ditopic diaminopyrrolic structures featuring unprecedented recognition properties toward the glycosides of the Manα(1–2)Man dimannoside. The results assess the new structures as the first receptors reported in the chemical literature capable of effectively recognizing dimannosides in polar organic media. Although admittedly recognition in water could not be evaluated, due to the insolubility of the receptors, we believe that the described structures represent a significant leap in the recognition of biologically relevant oligomannosides.

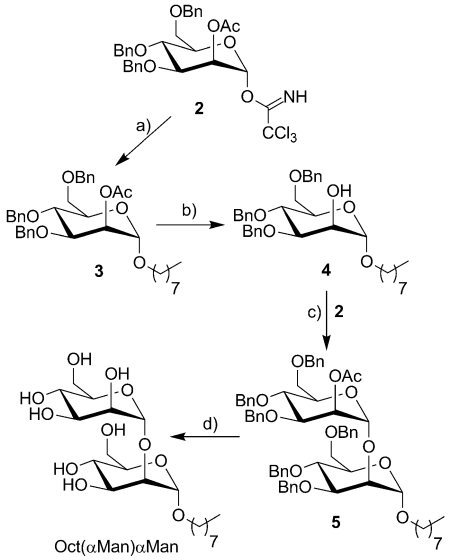

Scheme 1. Synthesis of *n*-octyl(α-D-mannopyranosyl)-(1→2)-α-D-mannopyranoside (Oct(αMan)αMan). Reagents and conditions: a) *n*-octanol, trimethylsilyl trifluoromethanesulfonate (TMSOTf), CH_2Cl_2, 0 °C, 15 min, 61 %; b) CH_3ONa 1 M solution in CH_3OH, RT, 45 min, 95 %; c) compound **2**, TMSOTf, CH_2Cl_2, 0 °C, 50 min, 60 %; d) CH_3ONa 1 M solution in CH_3OH, RT, 1.5 h, then H_2, $[Pd(OH)_2]/C$, CH_2Cl_2/CH_3OH 1:1, RT, 16 h, 84 %. Bn = benzyl.

Results and Discussion

Design: Having available a family of structures effectively recognizing monomannosides, the logical evolution of our studies involved choosing biologically relevant dimannosidic targets and modifying the architecture of the receptors to optimize the affinities and the selectivities toward the chosen dimannosides. Because the Manα(1–2)Man motif is encountered in important recognition processes, the α- and β-octyl glycosides of the Manα(1–2)Man dimannoside (Oct(αMan)αMan and Oct(αMan)βMan) were chosen to test the binding abilities of the modified structures, whereas the diaminopyrrolic receptor **1**, which was prepared in both enantiomerically pure forms[17] and gave best recognition results with the related monomannosides OctαMan and Octβ Man,[16] was selected as the appropriate building block to construct modified architectures.

The design of the receptors was based on the idea of bridging two units of **1** by an appropriate linker to build a ditopic structure capable of recognizing the two mannose units of the dimannoside through a tweezer-like architecture. Because markedly different recognition properties were exhibited by the two enantiomers of **1** toward Octβ Man, the derived ditopic receptors were also expected to show selectivity in the recognition of the dimannosides and were thus prepared in both enantiomerically pure forms for recognition studies.

Synthesis of glycosides: Because Oct(αMan)αMan and Oct(αMan)βMan were not commercially available, the target glycosides were prepared as described in Schemes 1 and 2.

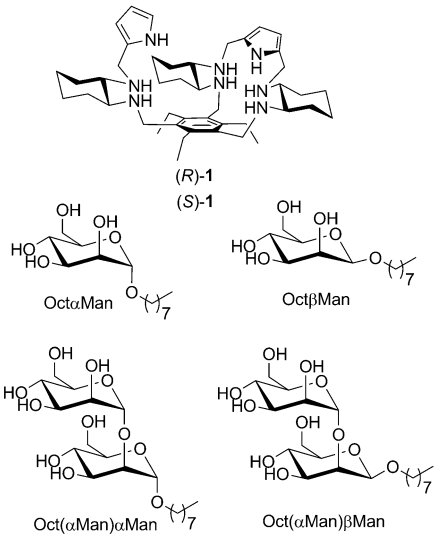

The octyl chain was necessary to ensure the solubility in polar organic solvents required for binding measurements.

The synthesis of the α-octyl glycoside was achieved by a standard glycosidation procedure. The trichloroacetimidate **2**[18] was glycosidated with *n*-octanol, deacetylated, and glycosylated on the free hydroxyl group with a second equivalent of compound **2**. The resulting α-dimannoside was deprotected to the desired Oct(αMan)αMan in good yields (see Scheme 1 for yields, reagents, and conditions).

For the synthesis of the β-octyl glycoside, because of the well-known difficulty of obtaining β-mannosides, Oct(αMan)βMan was prepared through the intramolecular agly-

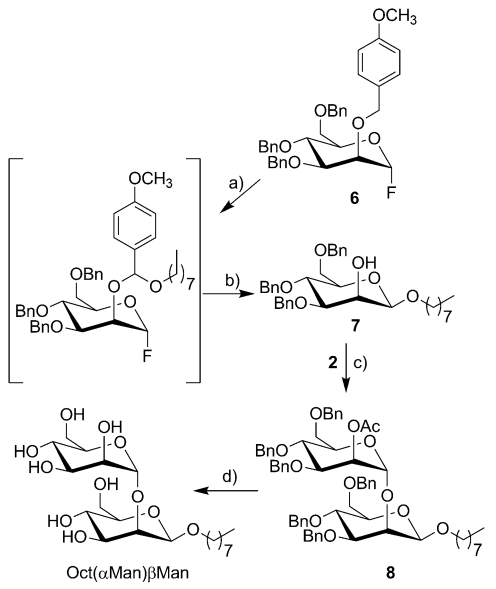

Scheme 2. Synthesis of *n*-octyl(α-D-mannopyranosyl)-(1→2)-β-D-mannopyranoside (Oct(αMan)βMan). Reagents and conditions: a) *n*-octanol, 2,3-dichloro-5,6,-dicyano-1,4-benzoquinone (DDQ), CH_2Cl_2, RT, 1 h; b) 2,6-di(*tert*-butyl)-4-methylpyridine (DTBMP), AgOTf (Tf = triflate), $SnCl_2$, CH_2Cl_2, RT, 3.5 h, 72%; c) compound **2**, TMSOTf, CH_2Cl_2, 0°C, 1 h, 63%; d) K_2CO_3, CH_3OH, RT, 3 h, then H_2, $[Pd(OH)_2]/C$, CH_2Cl_2/CH_3OH 1:1, RT, 16 h, 71%.

cone delivery (IAD) procedure.[19] The mannosyl fluoride **6**[20] was reacted with *n*-octanol under oxidative conditions to give the benzylic octylacetal intermediate. The latter transposed under Lewis acidic catalysis to deliver the octyl aglycone to the anomeric position from the same face, stereoselectively giving the β-glycoside **7** in good overall yields. Compound **7** was subsequently glycosylated on the free hydroxyl group with compound **2** and deprotected to Oct(αMan)βMan through the same procedure described for the corresponding α anomer (see Scheme 2 for yields, reagents and conditions).

Synthesis of the receptors: The ditopic receptor **9**, featuring a single carbon linker, could be prepared by condensing the dipyrrylmethane dialdehyde **10**[21] with the aminic precursor **11**[16a] of the monotopic receptor **1**, and reducing the resulting Schiff base with $NaBH_4$ (see Scheme 3). The *gem*-dimethyl group in the linker induces a convenient twisting of the two pyrrolic moieties of the dialdehyde **10**,[22] and presumably of the two halves of the ditopic structure as well, which may appropriately match the twist of the two mannose units of the dimannoside.[23] On the other hand, the single carbon hinge may impose conformational restrictions to the structure, which may hinder ligand binding.

The more flexible CH_2NHCH_2 bridging moiety was thus implemented in the structure of compound **12**, which was prepared by condensation of compound **11** with the corresponding dialdehyde **13**, followed by reduction of the Schiff base (Scheme 3). In addition to providing a more flexible linker, the hydrogen-bonding ability of the aminic group may result beneficial to the recognition properties of the structure. The dialdehyde **13** was prepared by condensing. the mono-protected pyrroledialdeyde **14**[24] with ammonia, reducing the Schiff base, and subsequently deprotecting the formyl groups (Scheme 4).

The rigid, non-hydrogen bonding, *p*-xylyl moiety implemented in the structure of compound **15** served as a reference to evaluate the impact of the hydrogen-bonding groups in the linker of the previous structures and the role of the size and the rigidity of the bridging moiety. Receptor **15** was prepared from terephthalaldehyde following the general procedure shown in Scheme 3.

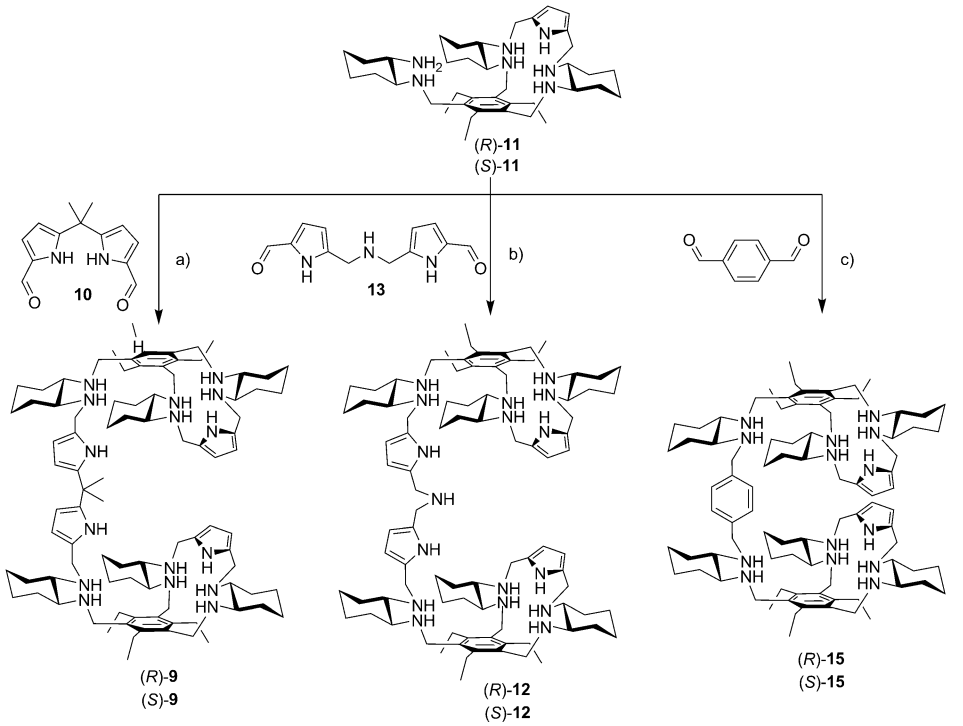

Scheme 3. Synthesis of receptors **9**, **12**, and **15** from enantiomerically pure (*R*)- and (*S*)-**11**. Reagents and conditions: a) 5,5′-(propane-2,2-diyl)bis(1*H*-pyrrole-2-carbaldehyde), $CHCl_3$, 70°C, 3 h, then $NaBH_4$ suspension in CH_3OH, RT, 3 h, 46%; b) compound **13**, $CHCl_3$, RT, 18 h, then $NaBH_4$ suspension in CH_3OH, RT, 3 h, 40%; c) terephthalaldehyde, $CHCl_3$, RT, 18 h, then $NaBH_4$ suspension in CH_3OH, RT, 4 h, 58%.

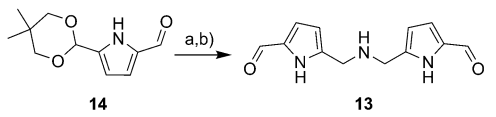

Scheme 4. Synthesis of linker **13**. Reagents and conditions: a) NH_3, CH_3OH, 60 °C, 3 h, then $NaBH_4$, RT, 2 h, then compound **14**; CH_3OH, RT, 3 h, then $NaBH_4$, RT, 2 h, 80 %; b) HCl 1 M, H_2O, RT, 2.5 h, 72 %.

Eventually, a receptor featuring the narrowest cleft of the set was obtained by replacing the diaminocyclohexane fragment of the pyrrolic bridge with a simple amine moiety in structure **16**. The latter would provide information on the cleft size required for the binding to a disaccharidic ligand. Receptor **16** was prepared starting from the dibromo-monoazido reactant **17**[25] as described in Scheme 5. Compound **17** was reacted with sodium acetate, and the resulting diacetate was hydrolyzed to the diol and oxidized to the dialdehyde **18** by pyridinium chlorochromate (PCC). The dialdehyde was condensed with the mono-BOC-protected diaminocyclohexane and the Schiff base was reduced and deprotected

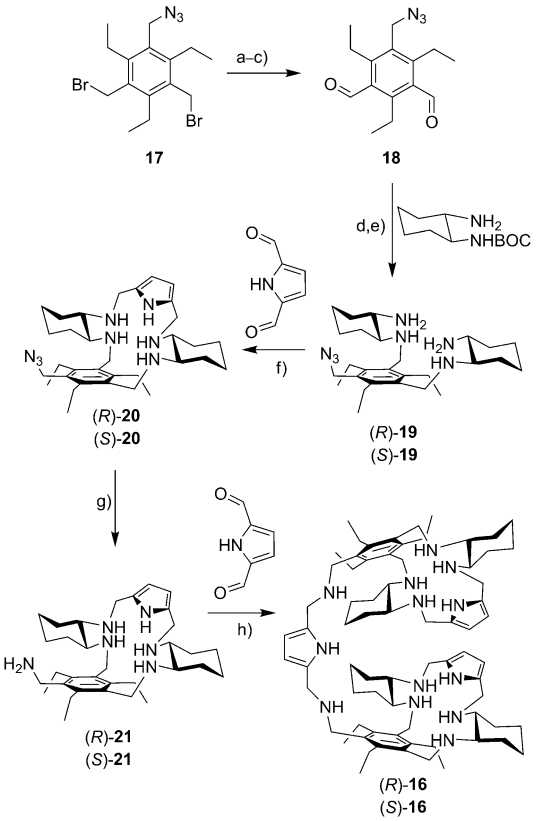

Scheme 5. Synthesis of receptor **16**. Reagents and conditions: a) AcONa, DMF, 100 °C, 2 h, >99 %; b) K_2CO_3, CH_3OH, RT, 70 h, >99 %; c) pyridinium chlorochromate, CH_2Cl_2, RT, 2 h, 95 %; d) *N-tert*-butoxycarbonyl-1,2-diaminocyclohexane, $CHCl_3$, 80 °C, 15 h, then $NaBH_4$, CH_3OH, RT, 3 h, >99 %; e) trifluoroacetic acid (TFA), CH_2Cl_2, RT, 3 h, 63 %; f) pyrrole-2,5-dicarbaldehyde, $CHCl_3$, RT, 15 h, then $NaBH_4$, CH_3OH, RT, 1.5 h, 96 %; g) PhP_3, H_2O, THF, RT, 15 h, 87 %; h) pyrrole-2,5-dicarbaldehyde, $CHCl_3$, RT, 15 h, then $NaBH_4$, CH_3OH, RT, 1 h, 70 %. BOC = *tert*-butoyloxycarbonyl.

to the tetramine **19**. The latter was condensed with 2,5-diformyl pyrrole and reduced to the tetraminopyrrolic intermediate **20**, featuring the cyclic unit of the receptor. Staudinger reduction of the azide, followed by further condensation with 2,5-diformyl pyrrole gave, after reduction of the Schiff base, the ditopic receptor **16**.

To obtain enantiopure receptors of opposite chirality, all the described syntheses were performed starting from the enantiopure diaminocyclohexane reagents of (*R*,*R*) and (*S*,*S*) configuration, providing structures of all-*R* and all-*S* configuration, respectively.

It should be noted that the designed structures are conformationally flexible, thus, not preorganized in a tweezer-like conformation. This conformation may be achieved upon complexation if the correct binding geometry would provide the required energy gain. Improved binding capabilities with respect to the monotopic receptors would therefore suggest a convergent arrangement of the two units into a tweezer-like conformation and would support the efficacy of the modular design.

Recognition studies: To assess the improvement achieved through the described structure modifications, the affinities of the ditopic receptors for Oct(αMan)αMan and Oct(αMan)βMan were determined in a polar organic medium. Association constants were measured by ^{1}H NMR spectroscopic titrations according to a previously described protocol,[26] which consists in the simultaneous fit of the complexation induced shifts[27] of all the available signals from both the receptor and the glycoside to the appropriate association model by nonlinear regression analysis.

The main issue to be addressed in this study was the selection of an appropriate medium that would provide the solubility of both reactants required for binding measurements, as the dimannosides were soluble in strongly polar solvents, whereas the receptors were soluble in solvents of low permittivity, but not in water. A mixture of $CDCl_3$ and DMF turned out to be the medium of choice, ensuring an overlap of the solubility ranges by allowing the appropriate tuning of the polarity by simply changing their mole ratio. We found that 30 % of DMF in $CDCl_3$ (v/v) was an appropriate polar medium to run the whole set of measurements. We also found that binding constants measured in this medium were comparable to those measured in acetonitrile, when using the values obtained in the latter solvent for the binding of **1** to monomannosides as reference,[16a] giving an indication of the competitivity of the medium, which can be useful to compare results with previous data. The results obtained for receptors **9**, **12**, **15**, and **16** with Oct(αMan)αMan and Oct(αMan)βMan are reported in Table 1, together with those obtained for receptor **1** and with OctαMan and Octβ Man for a direct comparison of the binding properties of mono- versus ditopic receptors, and of mono- versus dimannosides in the same medium.

Because multiple complex species were found in most cases, affinities were assessed from the measured binding constants through the BC_{50}^0 parameter, a binding descriptor

Table 1. Cumulative formation constants ($\log\beta$)[a] and intrinsic median binding concentration (BC_{50}^0)[b] for receptor to glycoside (R/G) complexes of octyl mannosides and octyl dimannosides in $CDCl_3$/DMF 70:30.

Receptor[c]	OctαMan		OctβMan		Oct(αMan)αMan		Oct(αMan)βMan	
	$\log\beta$ (R/G)	BC_{50}^0 [μM]	$\log\beta$ (R/G)	BC_{50}^0 [μM]	$\log\beta$ (R/G)	BC_{50}^0 [μM]	$\log\beta$ (R/G)	BC_{50}^0 [μM]
(*R*)-**1**	(3.41±0.02) (1:1) (5.83±0.06) (2:1) (4.96±0.17) (1:2)	(352±18)	(2.66±0.07) (1:1) (4.70±0.08) (2:1) (4.80±0.06) (1:2)	(1453±128)	(2.76±0.04) (1:1) (4.51±0.09) (2:1)	(1585±140)	(2.49±0.09) (1:1) (5.04±0.02) (2:1)	(1908±166)
(*S*)-**1**	(3.59±0.02) (1:1) (6.13±0.05) (2:1) (4.93±0.21) (1:2)	(238±9)	(3.56±0.08) (1:1) (6.51±0.09) (2:1)	(228±29)	(3.15±0.05) (1:1) (5.84±0.07) (2:1)	(556±47)	(3.00±0.07) (1:1) (5.16±0.12) (2:1)	(890±112)
(*R*)-**9**	(2.380±0.003) (1:1)	(4173±28)	(2.39±0.03) (1:1) (4.95±0.04) (2:1)	(2253±86)	(3.03±0.01) (1:1)	(940±3)	(2.88±0.01) (1:1)	(1324±31)
(*S*)-**9**	(2.82±0.03) (1:1) (4.71±0.12) (1:2)	(1289±82)	(3.00±0.08) (1:1) (5.29±0.15) (1:2)	(782±100)	(3.49±0.08) (1:1) (5.56±0.50) (2:1)	(311±54)	(4.80±0.10) (1:1) (8.28±0.17) (2:1)	(15±3)
(*R*)-**12**	(3.24±0.04) (1:1) (5.41±0.07) (1:2)	(504±38)	(3.32±0.07) (1:1) (5.86±0.09) (1:2)	(386±43)	(3.11±0.14) (1:1) (6.42±0.11) (2:1)	(420±58)	(3.50±0.06) (1:1) (5.73±0.28) (2:1)	(299±39)
(*S*)-**12**	(3.56±0.07 (1:1) (6.05±0.10) (1:2)	(242±30)	(3.66±0.08) (1:1) (6.12±0.17) (1:2)	(200±30)	(3.63±0.06) (1:1) (7.75±0.08) (2:1)	(101±8)	(4.19±0.04) (1:1) (10.39±0.16) (2:2)	(64±6)
(*R*)-**15**	(2.228±0.002) (1:1)	(5913±33)	(2.020±0.002) (1:1)	(9541±53)	(2.75±0.03) (1:1) (5.35±0.10) (1:2)	(1023±76)	(2.524±0.009) (1:1)	(2993±61)
(*S*)-**15**	(2.76±0.01) (1:1) (3.99±0.28) (1:2)	(1659±73)	(2.554±0.001) (1:1)	(2796±8)	(3.15±0.08) (1:1) (5.21±0.32) (2:1)	(662±108)	(2.81±0.01) (1:1) (4.66±0.03) (1:2)	(1332±30)
(*R*)-**16**	(2.97±0.06) (1:1) (5.27±0.11) (1:2)	(828±86)	(2.94±0.02) (1:1) (5.88±0.05) (2:1)	(709±30)	(3.16±0.04) (1:1) (5.22±0.15) (1:2)	(613±46)	(3.30±0.02) (1:1) (5.64±0.10) (1:2)	(430±21)
(*S*)-**16**	(3.30±0.04) (1:1) (5.81±0.19) (1:2)	(407±26)	(3.12±0.03) (1:1) (5.04±0.18) (1:2)	(681±46)	(3.40±0.05) (1:1) (5.75±0.1)6 (2:1)	(368±37)	(3.45±0.04) (1:1) (6.43±0.11) (1:2)	(250±20)

[a] Measured by ^{1}H NMR spectroscopy (400–900 MHz) from titration experiments at $T = 298$ K. Formation constants were obtained by nonlinear least-square regression analysis of the NMR data by simultaneous fit of all available signals from both reagents. [b] Calculated from the log β values by using the "BC_{50} Calculator" program (see ref. [28]). [c] See reference [17].

that quantitatively defines the overall affinity of a receptor for a ligand.[29] The BC_{50}^0 values calculated for the investigated systems through the "BC_{50} Calculator"[28] are also reported in Table 1. Gratifyingly, it can be appreciated that all the ditopic receptors consistently bound the dimannosides more effectively than the monomannosides, whereas the opposite was true for the monotopic receptor **1**.

Although the design of the ditopic receptors appeared well suited for the recognition of the disaccharides, the results clearly showed that the bridging arm played a crucial role. Receptor **15**, featuring the *p*-xylyl moiety in the linker, gave the worst results of the set showing, with a single exception, affinities in the millimolar range toward both mono- and dimannosides. On the contrary receptor **9**, featuring a dipyrrolic bridge, gave the best affinity of the whole set, showing toward the β-dimannoside a BC_{50}^0 value in the low micromolar range. Even more interestingly, the β-dimannoside was recognized by the chiral receptor with an outstanding enantioselectivity, the (*S*) enantiomer being more effective than the (*R*) enantiomer by nearly two orders of magnitude. On the other hand, the best affinity for the α-dimannoside was shown by receptor **12**; the latter gave excellent BC_{50}^0 values for both dimannosides, but showed rather shallow enantioselectivity and α/β discrimination.

The above-discussed results indicate a substantial contribution to the recognition from the pyrrolic groups of the linker, where the twisted bridge of receptor **9** appears to be determinant for the matching of the enantiomers to the ligand, whereas the more flexible linker of **12** seems to favor the adaptivity of the receptor at the expenses of selectivity. In agreement with these conclusions, receptor **16** behaves much like receptor **12**, although exhibiting weaker affinities: most likely, the smaller size of the flexible, monopyrrolic bridge does not affect the binding capabilities of **16**, but the lack of one of the two pyrrolic rings results in increased BC_{50}^0 values. Altogether, bridging monotopic binding units with a linker of appropriate size and flexibility and endowed with effective binding groups proved to be a successful strategy.

To confirm the interesting results obtained, we challenged the binding abilities of the best performing receptors **9** and **12** toward Oct(αMan)αMan and Oct(αMan)βMan in a more competitive medium. To this end, the amount of DMF in the mixture was raised to 40% and the extent of the weakening effect of the increased polar solvent on the affinities was assessed by replicating the NMR spectroscopic titrations. A typical example is depicted in Figure 1, in which a marked shift of the signals of both reactants is evident, showing that binding of (*S*)-**9** to Oct(αMan)βMan is still substantial in the more competitive medium. Because multiple complex species were still detectable, to avoid ambiguities in the definition of the equilibrium model, two independent titrations at different concentrations of the reactants were performed for each receptor/ligand system investigated, and the two set of data were simultaneously fitted including all available signals from both the receptor and the dimannoside. This approach drastically reduced the correlation of the data, providing well-defined models and reliable binding constants. The results obtained are shown in

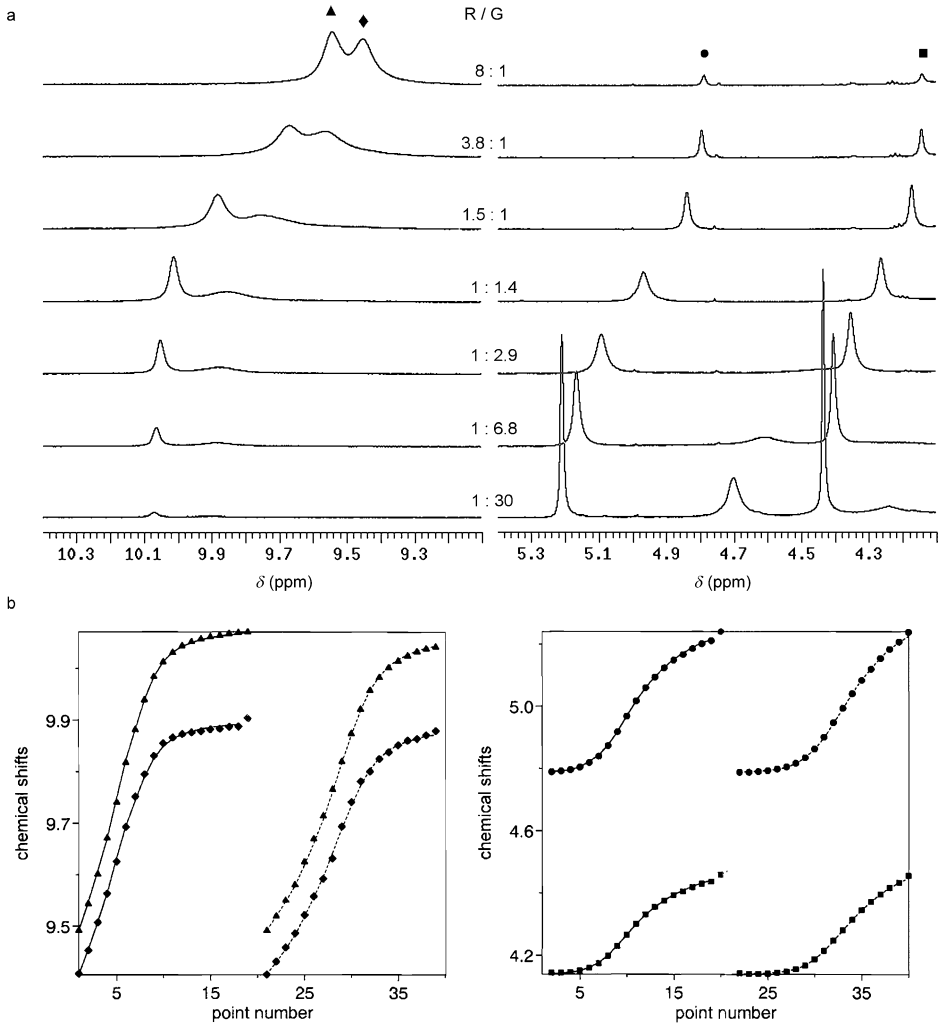

Figure 1. ^{1}H NMR spectroscopic titrations (400 MHz, $CDCl_3$/DMF 60:40, 298 K) of Oct(αMan)βMan (12.7 mM, set 1; and 6.03 mM, set 2) with (*S*)-**9** (12.5 mM). a) Selected spectral regions from the ^{1}H NMR spectra of a single titration (set 1) showing the signal shifts observed for an increasing receptor to glycoside (R/G) mole ratio. Representative signals of the receptor (left) and of the glycoside (right) are reported: ▲ NH-Pyrr′ (endocyclic pyrrole), ◆ NH-Pyrr (exocyclic pyrrole), ● CH-1a (αMan anomeric proton), ■ CH-1 (octyl βMan anomeric proton). b) Plot of the complexation-induced shifts of the corresponding receptor (left) and glycoside (right) proton signals along the titrations. Symbols are experimental data points; lines (—— set 1, ----- set 2) are best fit curves obtained through nonlinear regression by simultaneous fit of all available signals from the two independent titrations at different reactant concentrations.

Table 2, where the measured binding constants and the calculated BC_{50}^0 values for receptors **9** and **12** toward the two dimannosides are reported. Comparison of the results with the corresponding data from Table 1 shows, apart from the expected affinity decrease, that the binding abilities follow essentially the same trend in the two different media, featuring the (*S*) enantiomers performing better than the (*R*) enantiomers for both receptors, although exhibiting better selectivities for receptor **9** and higher affinities for receptor **12**. What appears to suffers the most from the more competitive medium is the selectivity; indeed, the main difference appears to be the shallower enantiomeric as well as anomeric discrimination, the larger affinities being affected more heavily than the smaller ones. Nevertheless, micromolar affinities are still monitored in most cases, indicating that recognition properties tolerate well the increasing competition from the medium.

The binding affinities obtained by NMR spectroscopy were further confirmed by isothermal titration calorimetry (ITC), as an independent technique, in 40% DMF in $CHCl_3$. The issue of the presence of multiple complex species was addressed through the same approach followed for the NMR data, by combining independent titrations run at different reactant concentrations into a simultaneous fit of all data, when necessary to remove ambiguities in the definition of the model. The ITC results of (*S*)-**9** with Oct(αMan)βMan are reported in Figure 2 as an illustrative case, to be compared to the corresponding NMR spectroscopic titration and data treatment displayed in Figure 1. The binding constants measured by ITC and the BC_{50}^0 values calculated for receptors **9** and **12** with Oct(αMan)αMan and Oct(αMan)βMan are reported in Table 3.

Comparison of the observed affinities with those obtained by NMR spectroscopy shows a generally good agreement, although not excellent in all cases. The discrepancy is clearly apparent in the models detected from the two techniques, as up to four binding constants were measured by NMR spectroscopy, whereas no more than two could be obtained by ITC. Such a discrepancy can be ascribed to the higher definition of the equilibrium systems that can be obtained by NMR spectroscopy with respect to ITC, because the larger number of data points (many shift data for several signals of both reactants) and the higher sensitivity of the shift modulation to the presence of different complex species, allow for a much finer deconvolution of the binding isotherm by the former technique. As a result, the number of species (and therefore of binding constants) that can be appreciated by ITC is limited by the intrinsic resolution of the technique.[30]

However, taking into account the formation constants for the 1:1 complexes, which give the most relevant contribution

Table 2. Cumulative formation constants[a] and intrinsic median binding concentration[b] for receptor to glycoside (R/G) complexes of octyl dimannosides in $CDCl_3$/DMF 60:40 from NMR spectroscopic data.

Receptor	Oct(αMan)αMan		Oct(αMan)βMan	
	logβ (R/G)	BC_{50}^0 [μM]	logβ (R/G)	BC_{50}^0 [μM]
(*R*)-**9**	(2.31±0.04) (1:1)	(3743±310)	(2.23±0.02) (1:1)	(3376±73)
	(3.61±0.18) (1:2)		4.31±0.02) (1:2)	
	(6.34±0.24) (2:2)			
(*S*)-**9**	(2.92±0.03) (1:1)	(1103±75)	(3.23±0.19) (1:1)	(231±33)
	(4.79±0.07) (2:1)		(6.97±0.14) (2:1)	
	(3.74±0.34) (1:2)		(9.90±0.17) (2:2)	
(*R*)-**12**	(3.30±0.10) (1:1)	(387±58)	3.20±0.02) (1:1)	(540±19)
	(5.95±0.18) (2:1)		(5.71±0.03) (2:1)	
	(5.32±0.28) (1:2)			
	(8.73±0.35) (2:2)			
(*S*)-**12**	(3.48±0.08) (1:1)	(297±41)	(3.64±0.06) (1:1)	(212±25)
	(5.38±0.27) (2:1)		(6.18±0.11) (2:1)	
	(5.33±0.14) (1:2)			
	(9.15±0.17) (2:2)			

[a] Measured by ^{1}H NMR spectroscopy (400–900 MHz) from titration experiments at $T=298$ K. Formation constants were obtained by nonlinear least-square regression analysis of NMR data by simultaneous fit of all available signals from both reagents. [b] Calculated from the logβ values by using the "BC_{50} Calculator" program (see ref. [28]).

to the affinity, it can be clearly seen that the agreement between the NMR spectroscopic and the ITC values is very good indeed, the data for (*S*)-**12** showing the only significant deviation. Thus, within the discussed limits, the overall affinity pattern and the measured binding constants are essentially confirmed by the two independent techniques.

Structural studies: A description of the binding mode characterizing the investigated receptor–carbohydrate complexes in solution was attempted by combining NMR techniques with molecular modeling calculations. This approach was complicated by some basic issues affecting these systems: indeed, the occurrence of multiple complex species of comparable stability at room temperature prevented the identification of suitable conditions for an NMR spectroscopic investigation, which required the 1:1 complex to be the prevalent species; on the other hand, the structures of the receptors were too flexible to obtain well-defined energy minima in the conformational space of the investigated complexes. Fortunately, we found that titration data obtained at 50 °C could be adequately fitted to the 1:1 model, thus allowing the selection of conditions under which useful amounts of the desired complex could be formed in solution, despite the lower affinity of the receptor for the disaccharide at that temperature.

The complex of receptor (*S*)-**9** with Oct(αMan)βMan was selected as a representative system and its structural features were studied at 50 °C in $CDCl_3$/[D_7]DMF 60:40 by NMR techniques. Under these conditions, a logβ value of (2.51±0.04) was measured for the 1:1 complex from a titration of the glycoside with (*S*)-**9**, which would cause nearly 80 % of complex to be formed at a concentration of dimannoside and receptor of 5 and 15 mM, respectively, the free reactants accounting for the rest of the species in solution.

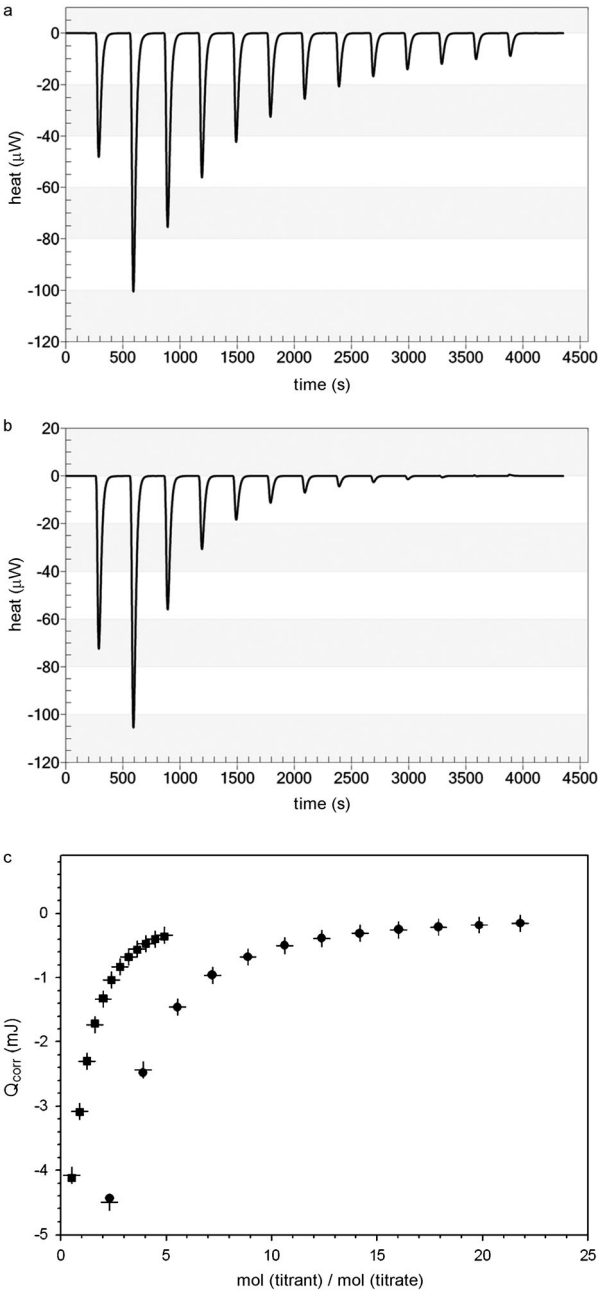

Figure 2. ITC results of Oct(αMan)βMan with (*S*)-**9** in $CDCl_3$/DMF 60:40 at $T=298$ K. a) Titration of (*S*)-**9** (0.48 mM) with Oct(αMan)βMan (7.71 mM). b) Titration of Oct(αMan)βMan (0.27 mM) with (*S*)-**9** (19.2 mM). c) Plot of the experimental data points for titrations a) (■) and b) (●). Crosshair symbols (+) are calculated points obtained by simultaneous fit of all data through nonlinear regression.

A further issue was the severe overlap of the saccharide signals with those of the receptor. This issue was addressed by following the proton resonances along the titration through HSQC 2D spectra, which deconvoluted the overlapped signals over the ^{13}C dimension and provided chemical shift variations for all dimannoside signals. Signal assignments were unambiguously obtained through HSQC, DQ-COSY, and TOCSY 2D spectra. The chemical shifts of the

Table 3. Cumulative formation constants[a] and intrinsic median binding concentration[b] for receptor to glycoside (R/G) complexes of octyl dimannosides in $CDCl_3$/DMF 60:40 obtained from the ITC data.

Receptor	Oct(αMan)αMan		Oct(αMan)βMan	
	logβ (R/G)	BC_{50}^0 [μM]	logβ (R/G)	BC_{50}^0 [μM]
(*R*)-**9**	(2.66±0.01) (1:1) (4.88±0.08) (2:1)	(1698±38)	(2.253±0.004) (1:1)	(5589±54)
(*S*)-**9**	(2.812±0.003) (1:1)	(1542±12)	(3.426±0.007) (1:1) (5.98±0.02) (2:1)	(335±4)
(*R*)-**12**	(3.16±0.01) (1:1) (5.82±0.02) (2:1)	(552±12)	(3.20±0.01) (1:1) (6.18±0.03) (2:1)	(445±11)
(*S*)-**12**	(3.90±0.02) (1:1) (7.12±0.09) (2:1)	(107±5)	(4.036±0.008) (1:1) (6.06±0.04) (2:1)	(91±2)

[a] Measured by ITC titration experiments at $T=298$ K. Formation constants were obtained by nonlinear least-square regression analysis of calorimetric data by simultaneous fit of combined titrations. [b] Calculated from the log β values using the "BC_{50} Calculator" program (see ref. [28]).

Table 4. Chemical shifts and chemical shift differences of the relevant protons of Oct(αMan)βMan free and Oct(αMan)βMan bound to (*S*)-**9** in the 1:1 complex in $CDCl_3$/[D_7]DMF 60:40 at $T=323$ K.[a]

Nucleus[b]	δ [ppm]		CSD [ppm]
	free	bound	
H-1a	4.6719	4.1694	0.5025
H-3a	3.1989	2.6143	0.5846
H-4a	3.1796	1.4186	1.7610
H-5a	3.5150	3.0325	0.4825
H-1	3.8998	3.5482	0.3516
H-2	3.4532	3.1216	0.3316
H-4	3.0821	2.5815	0.5006
H-7′	3.2481	2.7940	0.4541
H-7′	2.8692	2.3697	0.4995

[a] Chemical shifts were obtained by nonlinear regression of the experimental data from titration of Oct(αMan)βMan with (*S*)-**9**. [b] Nuclei labeled with lower-case "a" belong to the αMan fragment of Oct(αMan)βMan.

free and bound dimannoside obtained from the titration are reported in Table 4; the corresponding chemical shift differences (CSD) are depicted in Figure 3.

It can be immediately seen that all protons experience an upfield shift caused by the aromatic shielding effect, indicating the inclusion of the dimannoside in the cleft of the receptor; most remarkably, the H-4a proton, showing an outstanding shift of nearly 2 ppm, which demonstrated its location in close proximity to the aromatic moiety of one of the two subunits of the receptor. This feature is analogous to that observed for the (*S*)-**1**/OctαMan complex, the binding mode of which was elucidated in a previous paper.[16b] This evidence suggested that modeling calculations may take advantage of the latter structure as a starting point for a conformational search on the (*S*)-**9**/Oct(αMan)βMan complex. The two dihedral angles about the α-glycosidic linkage, determining the relative orientation of the two monosaccharides, were also included among the constraints for the conformational search, by using the value reported in a study on the dimannoside conformation.[23a] The conformational search was then performed following a well-established molecular mechanics protocol (see the Supporting Information),[31] imposing, in a first approximation, the above constraints. The protocol returned a few families of structures, only one of which was in agreement with the observed chemical shift data (Figure S1 in the Supporting Information). The lowest-energy member of the family (eighteen structures were found within an energy window of 6.1 kJ mol^{-1}) was let to relax in a single-point energy minimization removing all constraints, resulting in the structure reported in Figure 4 as the global minimum.

Several intermolecular hydrogen bonds between pyrrolic/aminic NH groups of the receptor and OH groups of the disaccharide could be found in the structure of the complex, showing that both the monosaccharidic units are interacting with the monotopic subunits of the ditopic receptor. This feature

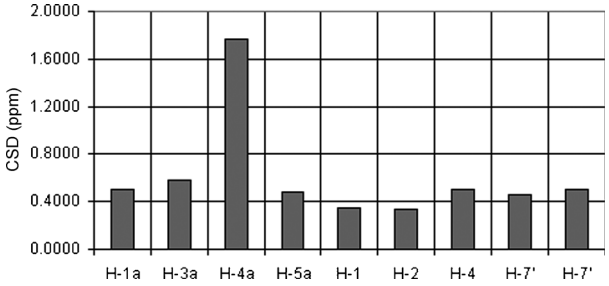

Figure 3. Plot of the chemical shift differences between free Oct(αMan)βMan and Oct(αMan)βMan bound to (*S*)-**9** in the 1:1 complex in $CDCl_3$/[D_7]DMF 60:40 at $T=323$ K.

not only accounts for the observed high affinity of (*S*)-**9** for Oct(αMan)βMan, but also explains the preference for dimannosides shown by the ditopic receptors with respect to their monotopic counterparts, therefore validating the modular design of our architectures.

An independent support to the calculated structure was obtained by NOESY spectra, that were run under the above-described conditions (Oct(αMan)βMan, 5 mM; (*S*)-**9**, 15 mM; $CDCl_3$/[D_7]DMF 60:40; $T=323$ K) (Figure 5). Intermolecular NOE cross peaks between the pyrrolic NH groups of the receptor and the CH protons of the saccharidic backbone were unambiguously detected in the 2D NOESY map, demonstrating the inclusion of the disaccharide in the receptor cleft. The interatomic distances calculated from the global minimum structure for the experimentally observed NOE contacts reported in Table 5 are in good agreement with a disposition of the α-mannosyl residue with

Table 5. Observed intermolecular NOE contacts and corresponding interatomic distances calculated from the global minimum structure of the complex of (*S*)-**9** with Oct(αMan)βMan.[a]

(*S*)-**9**	Oct(αMan)βMan (interatomic distance [Å])
NH-A	H-3a (3.80)
NH-B	H-1a (3.02)
NH-B	H-2a (3.54)

[a] From the 500 MHz NOESY spectrum of a 3:1 receptor-to-glycoside mixture in $CDCl_3$/[D_7]DMF 60:40 at $T=323$ K.

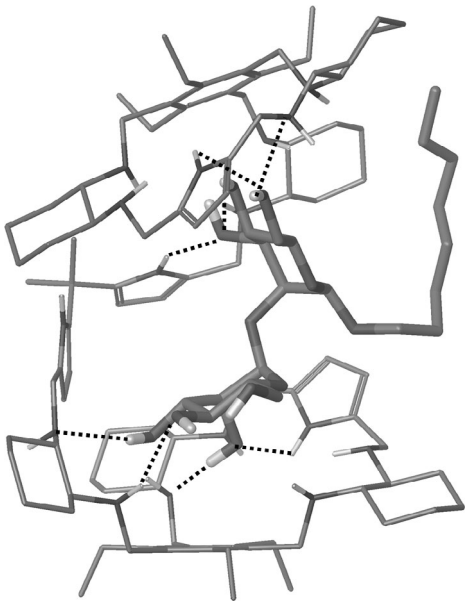

Figure 4. Global minimum structure obtained from a search of the conformational space for the complex between (*S*)-**9** and Oct(αMan)βMan. Hydrogen bonds involving pyrrolic and aminic NH groups are depicted as dashed lines. Selected hydrogen bond length [Å]: N–H(B)···OH-2a 2.48, O–H(2a)···NH 2.27, O–H(3a)···NH 2.30, N–H···OH-4a 2.27, N–H(A)···OH-3 2.15, N–H···OH-3 2.37, N–H(B)···OH-6 2.69, O–H(6)···NH 2.74. Nuclei labeled with lower-case "a" indicate the αMan fragment of Oct(αMan)βMan; NH-A/NH-B indicate the NH protons of the exocyclic and endocyclic pyrroles, respectively; NH indicate the aminic NH protons (see Figure 5).

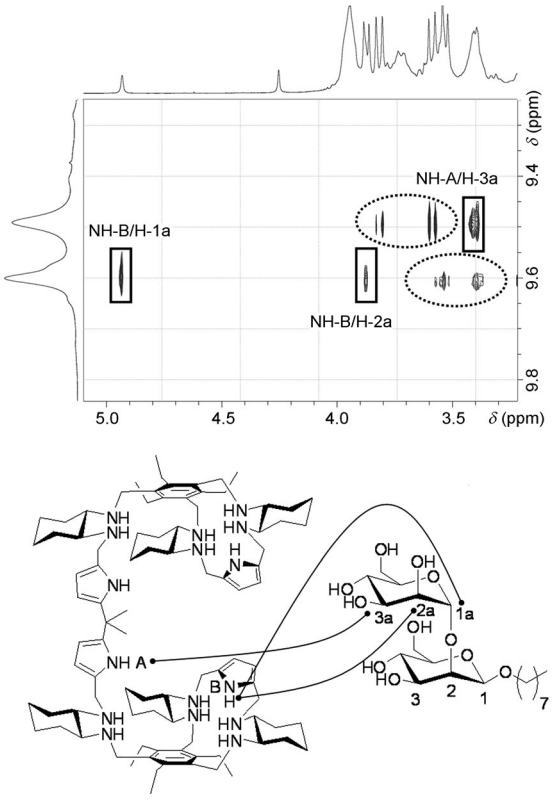

Figure 5. 500 MHz NOESY spectrum of a (*S*)-**9** to Oct(αMan)βMan 3:1 mixture in $CDCl_3$/[D_7]DMF 60:40 at $T = 323$ K. Intermolecular NOEs between the NH-A and NH-B protons (the NH protons of the exocyclic and endocyclic pyrroles, respectively) of (*S*)-**9**, and the H-1a, H-2a, and H-3a protons of the dimannoside are indicated by solid squares. Intramolecular NOEs of the receptor are indicated by dotted circles. A schematic representation of the intermolecular NOEs found between (*S*)-**9** and Oct(αMan)βMan is depicted on the bottom.

its β face over the aromatic scaffold, which causes the observed large shift of the H-4a proton, and confirms the consistency between the calculated structure and the combined NMR experimental data. The NOE cross peaks between the βMan fragment of Oct(αMan)βMan and the other subunit of the receptor, which could be expected from the global minimum structure, could not be identified unambiguously because of the severe overlap of inter- and intramolecular cross peaks from the reacting partners.

Finally, further support to the calculated structure is provided by the NOE contact observed between the H-1a and the H-2 protons of the dimannoside (Figure S2 in the Supporting Information), which is in agreement with the dihedral angles about the glycosidic linkage between the two mannose units obtained from the global minimum structure. We believe that the calculated structure gives a close description of the actual binding mode characterizing the molecular recognition of the dimannosides by ditopic aminopyrrolic receptors.

Conclusion

The results described in this paper have clearly shown that bridging two units of an effective receptor for mannosides through an appropriately designed linker does indeed lead to new ditopic structures capable of recognizing biologically relevant dimannosides with improved affinities with respect to their monotopic counterparts. Among the structures prepared, receptors **9** and **12** gave the most interesting results, the (*S*) enantiomer of the former giving the highest selectivity toward Oct(αMan)βMan, the latter showing affinities toward both dimannosides in the micromolar range even in a very competitive polar solvent. In all cases, the (*S*) enantiomer proved to be more effective than the (*R*) enantiomer, demonstrating a distinct enantiodiscrimination of the dimannosides toward the ditopic structures.

A combined approach through NMR techniques and molecular modeling calculations to the complex between Oct(αMan)βMan and (*S*)-**9** provided a description of the binding mode characterizing the recognition of the investigated dimannosides by the newly designed ditopic receptors and also provided a rationale for the observed preference for dimannosides exhibited by the ditopic receptors compared to their monotopic counterparts.

Although highly polar and very competitive, the medium used in this study (30–40% DMF in chloroform) is still quite far from an aqueous medium, thus, admittedly, the observed recognition properties were not detected under bio-

mimetic conditions. Yet, the binding abilities exhibited by the ditopic receptors appear very promising for the future development of biomimetic recognition in a physiological medium. Considering that recognition of oligomannosides by artificial receptors is not documented in the chemical literature, the structures reported in this work enriched the carbohydrate recognition toolbox of hitherto unprecedented biomimetic receptors for dimannosides.

Acknowledgements

High-field NMR spectra were acquired at the Magnetic Resonance Center (CERM) facilities of the Università di Firenze. We thank M. Lucci for technical assistance. Ente Cassa di Risparmio di Firenze (Italy) is acknowledged for granting an ITC nano calorimeter (grant no. 2009.0576).

[1] a) *The Sugar Code: Fundamentals of Glycosciences* (Ed.: H.-J. Gabius), Wiley-VCH, Weinheim, **2009**; b) T. K. Lindhorst, *Essentials of Carbohydrate Chemistry and Biochemistry*, 3rd ed., Wiley-VCH, Weinheim, **2007**; c) *Carbohydrates in Chemistry and Biology, Part I, Vol. 2* (Eds.: B. Ernst, G. W. Hart, P. Sinaÿ), Wiley-VCH, Weinheim, **2000**; d) *Carbohydrates in Chemistry and Biology, Part II, Vol. 4* (Eds.: B. Ernst, G. W. Hart, P. Sinaÿ), Wiley-VCH, Weinheim, **2000**.

[2] a) M. Mazik, *RSC Adv.* **2012**, *2*, 2630–2642; b) S. Jin, Y. Cheng, S. Reid, M. Li, B. Wang, *Med. Res. Rev.* **2010**, *30*, 171–257; c) D. B. Walker, G. Joshi, A. P. Davis, *Cell. Mol. Life Sci.* **2009**, *66*, 3177–3191; d) A. P. Davis, *Org. Biomol. Chem.* **2009**, *7*, 3629–3638; e) M. Mazik, *Chem. Soc. Rev.* **2009**, *38*, 935–956; f) S. Kubik, *Angew. Chem.* **2009**, *121*, 1750–1753; *Angew. Chem. Int. Ed.* **2009**, *48*, 1722–1725; g) A. P. Davis T. D. James in *Functional Synthetic Receptors* (Eds.: T. Schrader, A. D. Hamilton), Wiley-VCH, Weinheim, **2005**, pp. 45–109.

[3] *Carbohydrates in Chemistry and Biology, Part II, Vol. 4* (Eds.: B. Ernst, G. W. Hart, P. Sinaÿ), Wiley-VCH, Weinheim, **2000**, pp. 533–609.

[4] S.-C. Cheng, L. A. B. Joosten, B.-J. Kullberg, M. G. Netea, *Infect. Immun.* **2012**, *80*, 1304–1313.

[5] T. B. Geijtenbeek, S. J. Van Vliet, E. A. Koppel, M. Sanchez-Hernandez, C. M. Vandenbroucke-Grauls, B. Appelmelk, Y. Van Kooyk, *J. Exp. Med.* **2003**, *197*, 7–17.

[6] a) T. B. Geijtenbeek, D. S. Kwon, R. Torensma, S. J. Van Vliet, G. C. van Duijnhoven, J. Middel, I. L. Cornelissen, H. S. Nottet, V. N. Kewal Ramani, D. R. Littman, C. G. Figdor, Y. Van Kooyk, *Cell* **2000**, *100*, 587–597; b) P. Y. Lozach, A. Amara, B. Bartosch, J. L. Virelizier, F. Arenzana-Seisdedos, F. L. Cosset, R. Altmeyer, *J. Biol. Chem.* **2004**, *279*, 32035–32045.

[7] S.-K. Wang, P.-H. Liang, R. D. Astronomo, T.-L. Hsu, S.-L. Hsieh, D. R. Burton, C.-H. Wong, *Proc. Natl. Acad. Sci. USA* **2008**, *105*, 3690–3695.

[8] R. Pejchal, K. J. Doores, L. M. Walker, R. Khayat, P.-S. Huang, S.-K. Wang, R. L. Stanfield, J.-P. Julien, A. Ramos, M. Crispin, R. Depetris, U. Katpally, A. Marozsan, A. Cupo, S. Maloveste, Y. Liu, R. McBride, Y. Ito, R. W. Sanders, C. Ogohara, J. C. Paulson, T. Feizi, C. N. Scanlan, C.-H. Wong, J. P. Moore, W. C. Olson, A. B. Ward, P. Poignard, W. R. Schief, D. R. Burton, I. A. Wilson, *Science* **2011**, *334*, 1097–1103.

[9] C. A. Bewley, *Structure* **2001**, *9*, 931–940.

[10] S. Shahzad-ul-Hussan, E. Gustchina, R. Ghirlando, G. Marius Clore, C. A. Bewley, *J. Biol. Chem.* **2011**, *286*, 20788–20796.

[11] H. Tanaka, H. Chiba, J. Inokoshi, A. Kuno, T. Sugai, A. Takahashi, Y. Ito, M. Tsunoda, K. Suzuki, A. Takenaka, T. Sekiguchi, H. Umeyama, J. Hirabayashi, S. Omura, *Proc. Natl. Acad. Sci. USA* **2009**, *106*, 15633–15638.

[12] Y. Nakagawa, Y. Masuda, K. Yamada, T. Doi, K. Takegoshi, Y. Igarashi, Y. Ito, *Angew. Chem.* **2011**, *123*, 6208–6212; *Angew. Chem. Int. Ed.* **2011**, *50*, 6084–6088.

[13] a) J. Balzarini, *Nat. Rev. Microbiol.* **2007**, *5*, 583–597; b) C. N. Scanlan, J. Offer, N. Zitzmann, R. A. Dwek, *Nature* **2007**, *446*, 1038–1045.

[14] H.-K. Lee, C. N. Scanlan, C.-Y. Huang, A. Y. Chang, D. A. Calarese, R. A. Dwek, P. M. Rudd, D. R. Burton, I. A. Wilson, C.-H. Wong, *Angew. Chem.* **2004**, *116*, 1018–1021; *Angew. Chem. Int. Ed.* **2004**, *43*, 1000–1003.

[15] a) B. Sookcharoenpinyo, E. Klein, Y. Ferrand, D. B. Walker, P. R. Brotherhood, C. Ke, M. P. Crump, A. P. Davis, *Angew. Chem. Int. Ed.* **2012**, *51*, 4586–4590; b) Y. Jiao, J. Zhang, L. Zhang, Z. Lin, C. He, C. Duan, *Chem. Commun.* **2012**, *48*, 6022–6024; c) H. Abe, Y. Chida, H. Kurokawa, M. Inouye, *J. Org. Chem.* **2011**, *76*, 3366–3371; d) M. Mazik, A. C. Buthe, *Org. Biomol. Chem.* **2009**, *7*, 2063–2071; e) M. Mazik, A. C. Buthe, *Org. Biomol. Chem.* **2008**, *6*, 1558–1568; f) Y. Ferrand, M. P. Crump, A. P. Davis, *Science* **2007**, *318*, 619–622; g) T. Reenberg, N. Nyberg, J. Ø. Duus, J. L. J. van Dongen, M. Meldal, *Eur. J. Org. Chem.* **2007**, 5003–5009; h) O. Rusin, K. Lang, V. Král, *Chem. Eur. J.* **2002**, *8*, 655–663; i) A. S. Droz, U. Neidlein, S. Anderson, P. Seiler, F. Diederich, *Helv. Chim. Acta* **2001**, *84*, 2243–2289.

[16] a) C. Nativi, O. Francesconi, G. Gabrielli, A. Vacca, S. Roelens, *Chem. Eur. J.* **2011**, *17*, 4814–4820; b) A. Ardá, F. J. Cañada, C. Nativi, O. Francesconi, G. Gabrielli, A. Ienco, J. Jiménez-Barbero, S. Roelens, *Chem. Eur. J.* **2011**, *17*, 4821–4829.

[17] In the present work, the *R* and *S* descriptors are used to designate the receptors of all-*R* and all-*S* absolute configuration of the six stereocenters, respectively.

[18] B. Richichi, C. Nativi, L. Luzzatto, R. Notaro, G. LaMarca, *Bioorg. Chem.* **2011**, *39*, 88–93.

[19] Y. Ito, T. Ogawa, *Angew. Chem.* **1994**, *106*, 1843; *Angew. Chem. Int. Ed. Engl.* **1994**, *33*, 1765.

[20] I. Cumpstey, A. J. Fairbanks, A. J. Redgrave, *Org. Lett.* **2001**, *3*, 2371–2374.

[21] J. B. Love, J. A. Blake, C. Wilson, S. D. Reid, A. Novak, P. B. Hitchcock, *Chem. Commun.* **2003**, 1682–1683.

[22] S. P. Mahanta, B. S. Kumar, S. Baskaran, C. Sivasankar, P. K. Panda, *Org. Lett.* **2012**, *14*, 548–551.

[23] a) D. Chen, Y. Yao, Z. Wei, S. Zhang, P. Tu, B. Liu, M. Dong, *Comput. Theor. Chem.* **2013**, *1010*, 45–52; b) T. Srikrishnan, M. S. Chowdhary, K. L. Matta, *Carbohydr. Res.* **1989**, *186*, 167–175.

[24] C. Nativi, M. Cacciarini, O. Francesconi, G. Moneti, S. Roelens, *Org. Lett.* **2007**, *9*, 4685–4688.

[25] K. Niikura, E. V. Anslyn, *J. Chem. Soc. Perkin Trans. 2* **1999**, 2769–2776.

[26] A. Vacca, C. Nativi, M. Cacciarini, R. Pergoli, S. Roelens, *J. Am. Chem. Soc.* **2004**, *126*, 16456–16465.

[27] All investigated systems showed time-averaged signals for the free and complexed species, due to fast exchange on the NMR spectroscopic time scale.

[28] BC_{50} Calculator is a computer program developed for PC platforms and is available for free upon request from the corresponding author. For a detailed description of the equations used by the program for computing BC_{50} and BC^0_{50}, see: A. Vacca, O. Francesconi, S. Roelens, *Chem. Rec.*, **2012**, *12*, 544–566.

[29] The BC^0_{50} (intrinsic median binding concentration) descriptor is defined as the total concentration of receptor necessary for binding 50% of the ligand when the fraction of bound receptor is zero, that is, when forming the first complex molecule. This value coincides with the dissociation constant K_d for 1:1 complexes, whereas it can be viewed as a "global" dissociation constant when more than one complex is present in solution. For a comprehensive account of the descriptor, see: A. Vacca, O. Francesconi, S. Roelens, *Chem. Rec.* **2012**, *12*, 544–566.

[30] It should be emphasized that thermodynamic parameters are even more severely affected than binding constants by a simplified

model, and should therefore be taken with great care (see the Supporting Information, Table S1).

[31] For examples of application of NMR techniques assisted by molecular modeling, see: a) J. Jiménez-Barbero, E. Dragoni, C. Venturi, F. Nannucci, A. Ardá, M. Fontanella, S. André, F. J. Cañada, H. J. Gabius, C. Nativi, *Chem. Eur. J.* **2009**, *15*, 10423 – 10431; b) M. Kolympadi, M. Fontanella, C. Venturi, S. André, H. J. Gabius, J. Jiménez-Barbero, P. Vogel, *Chem. Eur. J.* **2009**, *15*, 2861 – 2873; c) S. Mari, F. J. Cañada, J. Jiménez-Barbero, A. Bernardi, G. Marcou, I. Motto, I. Velter, F. Nicotra, B. La Ferla, *Eur. J. Org. Chem.* **2006**, 2925 – 2933; d) S. Mari, H. Posteri, G. Marcou, D. Potenza, F. Micheli, F. J. Cañada, J. Jiménez-Barbero, A. Bernardi, *Eur. J. Org. Chem.* **2004**, 5119 – 5225.

Received: December 3, 2012
Published online: July 9, 2013

